X-30

[redacted]

SECURITY INFORMATION

Copy 217
RM A52E01

[redacted]

NACA

RESEARCH MEMORANDUM

EFFECTS OF THREE TYPES OF BLUNT TRAILING EDGES ON THE AERODYNAMIC CHARACTERISTICS OF A PLANE TAPERED WING OF ASPECT RATIO 3.1, WITH A 3-PERCENT-THICK BICONVEX SECTION

By Duane W. Dugan

Ames Aeronautical Laboratory
Moffett Field, Calif.

[redacted]

NATIONAL ADVISORY COMMITTEE
FOR AERONAUTICS
WASHINGTON
July 22, 1952

[redacted]

3/9 98/13

[redacted]

NATIONAL ADVISORY COMMITTEE FOR AERONAUTICS

RESEARCH MEMORANDUM

EFFECTS OF THREE TYPES OF BLUNT TRAILING EDGES ON THE AERODYNAMIC CHARACTERISTICS OF A PLANE TAPERED WING OF ASPECT RATIO 3.1, WITH A 3-PERCENT-THICK BICONVEX SECTION

By Duane W. Dugan

SUMMARY

Effects of wing trailing-edge bluntness upon the aerodynamic characteristics of a wing-body combination have been experimentally investigated at Mach numbers ranging from 0.6 to 0.925 and from 1.2 to 1.7 for Reynolds numbers of 1.5 and 3.8 million. Modifications were made to the rear half of a basic plane tapered wing of aspect ratio 3.1 having a 3-percent-thick, circular-arc, biconvex section. Three types of trailing-edge shapes were used; namely, (1) constant thickness aft of midchord, with zero boattail angle; (2) constant thickness from midchord to seven-eights chord followed by constant slope to one-half maximum airfoil thickness at trailing edge, with boattail angle equal to trailing-edge angle of basic wing; and (3) one-half maximum thickness at trailing edge faired by means of a tangent to the biconvex surface, with boattail angle of 2°.

Results of the investigation show that employment of blunt trailing edges reduced or eliminated unstable pitching-moment characteristics exhibited by the basic wing-body combination at low lift coefficients and subsonic speeds. In particular, at the supercritical Mach numbers 0.9 and 0.925, neutral or slightly positive static longitudinal stability of the wing-body configuration was attained by using trailing-edge bluntness. Increases in lift-curve slope measured through zero lift were also obtained, although at the cost of increased minimum drag and decreased maximum lift-drag ratios.

Comparison of the aerodynamic characteristics of the three modified wing-body combinations indicates that for the given basic wing the trailing-edge thickness which gives the most improvement in pitching-moment characteristics with the least decrease in maximum lift-drag ratio

[redacted]

in the subsonic speed range is less than one-half maximum airfoil thickness, and that utilization of a large boattail angle is undesirable.

INTRODUCTION

Previous experimental investigation of the aerodynamic characteristics of a wing-body combination employing a plane tapered wing of aspect ratio 3.1 with a 3-percent-thick, circular-arc, biconvex section (reference 1) has shown undesirable pitching-moment characteristics near zero lift in the subsonic Mach number range, particularly for the supercritical Mach numbers 0.9 and 0.925. (The critical Mach number for this wing is approximately 0.83.) The phenomena were believed to be due to significant changes in chordwise loadings caused by the influence of the terminal shock wave. Results of investigations of airfoils at high subsonic speeds (references 2 and 3) demonstrated the achievement of more satisfactory pitching moments through changes to the airfoil thickness distribution which moved the point of maximum thickness rearward, thereby confining the adverse influence of the terminal shock wave to a smaller portion of the airfoil. In addition, it has been pointed out in reference 4 that advantages, including greater lift-curve slope, lower profile drag, and desirable structural features, are possible at supersonic Mach numbers with blunt trailing-edge airfoils. Consideration of such evidence led to the present investigation of the effects of trailing-edge bluntness on the aerodynamic properties of the 3-percent-thick biconvex-profile wing of reference 1.

In this investigation, no attempt was made to compare aerodynamic characteristics of the various wings on the basis of equivalent structural characteristics. Therefore, the term "optimum thickness" as used in the present report is based solely on the aerodynamic characteristics of a given 3-percent-thick wing modified to obtain various trailing-edge shapes and thicknesses without regard to the structural strengths which differed from one modification to the other. Furthermore, because of the small thickness ratio of the wing and the range of Mach numbers of this investigation, and because the modifications to the basic wing did not reduce maximum thickness nor include changes in the profile forward of the midchord, no reduction in minimum drag at supersonic speeds was anticipated for the blunt trailing-edge wings.

NOTATION

b wing span, feet

$\bar{c}$ mean aerodynamic chord $\left(\dfrac{\int_0^{b/2} c^2 dy}{\int_0^{b/2} c\, dy}\right)$

c	local wing chord, feet
l	length of body, including portion removed to accommodate sting, inches
$\frac{L}{D}$	lift-drag ratio
$\left(\frac{L}{D}\right)_{max}$	maximum lift-drag ratio
M	free-stream Mach number
p_o	free-stream static pressure, pounds per square foot
p_b	pressure at base of blunt trailing-edge wings, pounds per square foot
$\frac{p_b - p_o}{q}$	wing base-pressure coefficient
q	free-stream dynamic pressure, pounds per square foot
R	Reynolds number based on the mean aerodynamic chord, $\bar{c}$
r	radius of body, inches
r_o	maximum body radius, inches
S	total wing area, including area formed by extending leading and trailing edges to plane of symmetry, square feet
x	longitudinal distance from nose of body, inches
y	distance perpendicular to plane of symmetry, feet
α	angle of attack of body axis, degrees
C_D	drag coefficient $\left(\frac{\text{drag}}{qS}\right)$
C_L	lift coefficient $\left(\frac{\text{lift}}{qS}\right)$
C_m	pitching-moment coefficient referred to quarter point of mean aerodynamic chord $\left(\frac{\text{pitching moment}}{qS\bar{c}}\right)$

$\frac{dC_L}{d\alpha}$ slope of lift curve measured at zero lift, per degree

$\frac{dC_m}{dC_L}$ slope of pitching-moment curve measured at zero lift

APPARATUS

Wind Tunnel and Equipment

The experimental investigation was conducted in the Ames 6- by 6-foot supersonic wind tunnel. In this wind tunnel the Mach number can be varied continuously and the stagnation pressure can be regulated to maintain a given test Reynolds number. The air is dried to prevent the formation of condensation shocks. Further information is presented in reference 5.

The model was sting mounted in the tunnel, the diameter of the sting being about 82 percent of the diameter of the body base. A balance mounted on the sting support and enclosed within the body of the model was used to measure the aerodynamic forces and moments on the model. The balance was the 4-inch, four-component, strain-gage balance described in reference 6.

Models

A plan and a front view of the models and certain model dimensions are given in figure 1. The biconvex profile and the three trailing-edge modifications are illustrated in figure 2. The basic wing of circular-arc biconvex section (wing 1) was constructed of solid steel, and was modified by adding bismuth-tin alloy aft of the midchord points to obtain wings 2, 3, and 4. Wing 2 has constant thickness from midchord to trailing edge; wing 3 has constant thickness from midchord to the 87.5-percent chord point, followed by constant slope to one-half the maximum thickness at the trailing edge, with a boattail angle of 6.88° (same as included trailing-edge angle of wing 1); wing 4 has a trailing-edge thickness equal to that of wing 3, but employs a constant slope from trailing edge to a point of tangency on the biconvex surface with a boattail angle of 2.02°. The body spar was also of steel and was covered with aluminum to form the body contours. The surfaces of the body and wings were polished smooth. Other important geometric characteristics of the models are tabulated as follows:

Wings

Aspect ratio	3.1
Taper ratio	0.39
Airfoil section (streamwise)	3-percent thick circular-arc biconvex
Included angle at nose, degrees	6.88
Boattail angle, degrees	
Wing 2	0
Wing 3	6.88
Wing 4	2.02
Total area S, square feet	2.425
Mean aerodynamic chord $\bar{c}$, feet	0.944
Dihedral, degrees	0
Camber	None
Twist, degrees	0
Sweepback of 25-percent-chord station, degrees	11.4
Incidence, degrees	0
Distance, wing-chord plane to body axis, feet	0

Body

Fineness ratio (based upon length l, fig. 1)	12.5
Cross-section shape	Circular
Maximum cross-sectional area, square feet	0.1235
Ratio of maximum cross-sectional area to wing area	0.0509

TESTS AND PROCEDURE

The aerodynamic characteristics of the models with wings 2, 3, and 4 (as a function of angle of attack) were investigated for a range of Mach numbers from 0.6 to 0.925 and from 1.2 to 1.7, and Reynolds numbers of 1.5 and 3.8 million. Data for the model with wing 1 were obtained from reference 1 for comparison. In a few instances, as noted in the figures, data for a Reynolds number of 1.5 million were not obtained for wing 1; the substitution of data obtained at a Reynolds number of 2.4 million did not invalidate comparison with the modified wings, inasmuch as no appreciable difference could be observed between the data obtained for wing 1 at R=1.5 million and those obtained at R=2.4 million in the Mach number range concerned.

In addition to force measurements, wing base-pressure measurements were made by means of a static orifice installed in the trailing edge of each of the modified wings at approximately the 50-percent-semispan position of the right-hand wing panel.

Reduction of Data

The test data have been reduced to standard NACA coefficient form. Factors which could affect the accuracy of these results and the corrections applied are discussed in the following paragraphs.

Tunnel-wall interference.- Corrections to the subsonic results for effects of the tunnel walls resulting from lift on the model were made according to the methods of reference 7. The numerical values of these corrections (which were added to the uncorrected data) were:

$$\Delta\alpha = 0.57\ C_L$$
$$\Delta C_D = 0.0100\ {C_L}^2$$

No corrections were made to the pitching-moment coefficients.

The effects of constriction of the flow at subsonic speeds by the tunnel walls were taken into account by the method of reference 8. This correction was calculated for conditions at zero angle of attack and was applied throughout the angle-of-attack range. At a Mach number of 0.925, this correction amounted to a 3-percent increase in the Mach number over that determined from a calibration of the wind tunnel without a model in place.

For the tests at supersonic speeds, the reflection from the tunnel walls of the Mach wave originating at the nose of the body did not cross the model. No corrections were required, therefore, for tunnel-wall effects.

Stream variations.- Tests at subsonic speeds in the 6- by 6-foot supersonic wind tunnel of the present symmetrical models in both the normal and the inverted positions have indicated no stream curvature or inclination in the pitch plane of the model. No measurements have been made, however, of the stream curvature in the yaw plane. At subsonic speeds, the longitudinal variation of static pressure in the region of the model is not known accurately at present, but a preliminary survey has indicated that it is less than 2 percent of the dynamic pressure. No correction for this effect was made.

A survey of the air stream at supersonic speeds (reference 5) has shown stream curvature and stream inclination only in the yaw plane of the model. The effects of this curvature and inclination on the measured characteristics of the present models are not known, but are judged to be small according to the results of reference 9. The survey also indicated that there is a static-pressure variation in the test section of sufficient magnitude to affect the drag results. A correction was added to the measured drag coefficient, therefore, to account for the longitudinal buoyancy caused by this static-pressure variation. This correction varied from as much as -0.0007 at a Mach number of 1.3 to +0.0006 at a Mach number of 1.7.

Support interference.- At subsonic speeds, the effects of support interference on the aerodynamic characteristics of the models are not known. For the present tailless models, it is believed that such effects consisted primarily of a change in the pressure at the base of the model fuselage. In an effort to correct at least partially for this support interference, the base pressure of the model fuselage was measured and the drag data were adjusted to correspond to a base pressure equal to the static pressure of the free stream. These corrections were of the order of 2 percent of the measured drag at zero lift.

At supersonic speeds, the effects of support interference of a body-sting configuration similar to that of the present models are shown by reference 10 to be confined to a change in base pressure. The previously mentioned adjustment of the drag for base pressure, therefore, was applied at supersonic speeds. The corrections in these cases ranged, in general, from 6 percent of the measured drag at zero lift at $M = 1.2$ to 15 percent at $M = 1.7$. The corrected drag, consequently, is forebody drag.

RESULTS AND DISCUSSION

Figure 3 shows typical basic-data plots of aerodynamic characteristics obtained in this investigation for wing 4. Because of the slight asymmetry in the drag polars near zero lift for the lower Mach numbers, the values of drag at positive lift were used in subsequent figures. Subsequent figures do not, in general, show test points in order that comparisons may be made more clearly in respect to the various properties of the four wings. A comparison of the aerodynamic characteristics of the four wings is presented in figures 4, 5, 6, and 7. In figure 8, the wing base-pressure coefficients of the modified wings are compared at several subsonic and supersonic Mach numbers. Figure 9 shows the variation of lift-curve slope measured through zero lift with Mach number for each wing. The effect of Mach number upon lift at several angles of attack is given in figure 10; the same is done for drag in figure 11, and for pitching moment in figure 12.

Lift Characteristics

Appreciable increases in lift-curve slope measured at zero lift (fig. 9) in the ranges of Mach numbers investigated were obtained by substituting blunt trailing edges for the closed trailing edge of the basic wing (wing 1), particularly at the supercritical Mach numbers 0.9 and 0.925. This is attributed to reduction of separation at all speeds tested and to the additional reduction of the adverse effects of the terminal shock at the supercritical speeds through the rearward shift of the shock. Of the three types of blunt trailing edges tested, that represented by wing 4, which has a final trailing-edge thickness of one-half maximum airfoil thickness faired by means of a tangent to the biconvex surface, demonstrated the most satisfactory lifting properties in regard to lift-curve slope and variation of lift with Mach number. This suggests the desirability of using the smallest possible boattail angle in attaining the final trailing-edge thickness which the results indicate should be less than maximum section thickness.

Figures 9 and 10 show a marked scale effect on the lift characteristics of wing 1 at angles of attack less than 4° in the subsonic, supercritical speed range, an effect not observed for the modified wings. The decrease of lift-curve slope measured through zero lift for wing 1 at the higher subsonic speeds and lower Reynolds number indicates that a combination of boundary-layer and terminal-shock effects causes loss of lift. Increasing the Reynolds number to 3.8 million, or shifting the position of the terminal shock rearward by changing the thickness distribution to that of wing 2, 3, or 4, reduces the effects of separation and of recompression, resulting in more lift at small angles of attack. That the same effect is not observed at somewhat larger angles (as at $\alpha = 4^{\circ}$) is attributed to the change in the nature of the flow at these angles (fig. 10(a)). As first described in reference 3, an expansion at supersonic speeds around the sharp leading edge redirects the air to the surface of the wing, at which point an oblique shock turns the flow so that it follows the contour of the surface, with the result that separation is eliminated over a considerable distance aft of the leading edge.

Pitching-Moment Characteristics

Improvement of the pitching-moment characteristics of the basic wing by employing blunt trailing edges of the types represented by wings 2 and 4 is apparent in figure 5, particularly at the two highest subsonic Mach numbers and lower Reynolds number. Wing 3 produces pitching-moment properties generally less satisfactory in respect to static longitudinal stability than those of the basic wing at 1.5 million Reynolds number and lower subsonic Mach numbers; at the higher Reynolds number, these characteristics are slightly superior to those of wing 1 at subsonic speeds, but remain less desirable than those of the other two modified wings. At supersonic Mach numbers, the influence of trailing-edge thickness in determining pitching-moment characteristics is slight.

The mitigation of Mach number effects upon pitching-moment through the use of blunt trailing edges is shown in figure 12 where the variation of pitching moment with Mach number at several angles of attack is presented for each of the four wings. Wings 2 and 4 appear superior in this respect whereas wing 3 does not. (The trailing-edge thickness of wing 3 is the same as that of wing 4, but the boattail angle of the former is more than three times that of the latter.) The data indicate that the use of full bluntness is scarcely more advantageous than that of half bluntness as typified by wing 4 in reducing the Mach number effects just discussed.

The aberrant variations of pitching moment with lift of wings 1 and 3 in the subsonic speed range at the lower Reynolds number, in contrast to the more consistent trends at the higher dynamic scale, as shown by figure 5, merit a brief discussion.

In the case of the basic wing (wing 1), the rapid increase in positive pitching moment at small lift coefficients at the supercritical Mach numbers 0.9 and 0.925 and the lower Reynolds number can be explained as follows: Assume that at zero lift laminar flow exists over both upper and lower surfaces of the wing, but that transition to turbulent boundary-layer flow occurs ahead of the terminal shock on the upper surface at small angles of attack due to the pressure peak in the vicinity of the sharp leading edge. The pressure distribution over the upper surface, then, would resemble that obtained experimentally at supercritical speeds on a circular-arc airfoil with turbulent boundary layer, whereas the pressure distribution over the lower surface would be similar to that obtained with laminar flow in the boundary layer. Such pressure distributions are presented in reference 11 for a biconvex airfoil at 0° incidence, and show that the terminal shock wave produces a greater pressure rise in a shorter chordwise distance in the presence of a turbulent boundary layer than in the presence of a laminar boundary layer. This, then, would account for the development of negative lift over the rear of wing 1 at supercritical speeds and the lower Reynolds number, and explain both the increased positive pitching moment (fig. 5(a)), and the decrease in lift-curve slope (fig. 9(a)). Examples of such pressure distributions over an airfoil identical to that of wing 1 can be seen for angles of attack of 2° and 4° in reference 3.

At the higher Reynolds number of 3.8 million, it can be deduced from the data for wing 1 that turbulent boundary-layer flow occurs over the lower as well as the upper surface at small angles of attack, with the result that the negative lift described above is largely reduced or eliminated.

The pitching-moment characteristics of wing 3 at lift coefficients near zero for supercritical speeds at the lower Reynolds number are contrary to those of wing 1 (fig. 5), and thus require a different explanation. A clue to the paradox is given by the discontinuity in the profile of wing 3. In this wing, the upper and lower surfaces aft of the midchord point continue parallel to the chord plane as far rearward as the 87.5-percent-chord position, at which point they change direction by an angle of 3.44°. Such a profile is conducive to separation behind the discontinuity at low Reynolds numbers. That separated flow does prevail over both surfaces at the rear of wing 3, not only at zero lift but also at small angles of attack, in the subcritical speed range is indicated by the more positive pitching moments of this wing compared to those of wings 1, 2, and 4. However, as supercritical speeds are attained, the supersonic expansion around the discontinuity on the upper surface is probably of sufficient degree to reattach the flow there and produce greatly reduced pressures at even small angles of attack, as study of the data and schlieren observations of reference 3 indicates. The lower velocities on the lower surface of the wing at small angles of attack preclude the possibility of as complete reattachment, with the result that more positive lift is developed over the rear of the wing at supercritical speeds than at lower subsonic speeds. Such a phenomenon would explain both the rapid increase of lift and of diving moment with the advent of supercritical speeds at the lower Reynolds number shown by the data presented in figures 10(a) and 12(a), respectively.

At the higher Reynolds number, the flow over the upper rear surface of wing 3 would not be expected to differ significantly from that at the lower Reynolds number; on the other hand, the extent of the separation on the lower surface aft of the discontinuity would be expected to be largely reduced. The tendency in this event would be toward less lift and a decrease in diving moment. Comparison of the lift and the pitching moments of wing 3 at the two Reynolds numbers (figs. 10 and 12, respectively) shows this to be the case.

In view of the scale effects noted for wings 1 and 3 in the supercritical range of speeds, the limitations to the direct application of these wings, say to missile design where the dimensions are comparable to those of the models here investigated, are obvious. The test conditions at the two supercritical Mach numbers 0.9 and 0.925, and at the lower Reynolds number of 1.5 million are equivalent to flight of the test models at these same values of the parameters at approximately 40,000 feet above sea level. Wings 2 and 4 would not offer the same drastic problem of control at small lift coefficients in the subsonic supercritical speed range.

Drag Characteristics

As could be expected, the minimum drag of each of the blunt trailing-edge wings was considerably greater than that of the basic wing, both at subsonic and supersonic speeds. For wing 2 the drag increments were three to four times as large as for wing 4 at zero lift and at small angles of attack (fig. 11); in general, the drag of wing 3 resembled that of wing 4 except at supersonic speeds and the higher Reynolds number where the drag of wing 3 exceeded that of wing 2 in the higher Mach number range (fig. 11(b)).

The influence of the trailing-edge shapes of the modified wings in creating additional drag through the development of lower base pressures is shown in a qualitative way in figure 8. The decrease of base pressure coefficient with increasing supersonic Mach number shown in figure 8 is reflected in the diminishing difference between the drag coefficients of the modified wings and those of the basic wing as the Mach number increases beyond 1.2 (fig. 11). The phenomenon of decreasing base pressure coefficients with increasing angle of attack near zero, shown for wing 2 in figure 8 for subsonic speeds, serves to explain the unusual shape of the drag-polar curves of that wing near zero lift (fig.6).

Figure 6 shows that the increase of drag with lift is lower for the modified wings than for the basic wing, as could be deduced from noting the greater lift-curve slopes of the former. At lift coefficients of the order of 0.5, the drag coefficients of the blunt-trailing-edge wings are generally lower than that of the basic wing.

Maximum Lift-Drag Ratio

Figure 7 shows the relative magnitude of the maximum lift-drag ratios of the four wings for subsonic and supersonic Mach numbers. It is uncertain just how much of the difference observed between the values of the ratios at the two Reynolds numbers is due to scale effect and how much is due to the lack of complete definitiveness in the fairing of the individual lift-drag curves near the maximum values. The advantage of using less than full bluntness is obvious in respect to the achievement of the largest possible lift-drag ratios. The data indicate some slight superiority of wing 4 over wing 3 in comparing their respective lift-drag values.

At the highest Mach number of the present investigation (M = 1.7), there is an indication that at least for wings 3 and 4 the values of maximum L/D are increasing with further increase in Mach number; from reference 1, wing 1 showed no such tendency up to a Mach number of 1.9 and a Reynolds number of 2.4 million. This increase in $(L/D)_{max}$ is no doubt associated with the decrease in base drag with increasing supersonic Mach number shown in figure 8. It is possible that at Mach numbers higher than 1.7 the order of the values of $(L/D)_{max}$ for the nonblunt and for the modified wings might be reversed. Further investigation at higher Mach numbers than here presented is required before definite conclusions can be reached.

CONCLUDING REMARKS

From the data obtained in this investigation of the effects of blunt trailing edges upon the aerodynamic characteristics of a plane tapered wing having a 3-percent-thick, circular-arc, biconvex section, it has been found that unstable pitching-moment characteristics exhibited by the above wing at small lift coefficients in the subsonic range of speeds considered can be reduced or eliminated. This was accomplished (at the cost of increased drag and lower maximum lift-drag ratios) by the employment of trailing edges having thicknesses equal to the maximum and one-half the maximum thickness of the wing. Increases in lift-curve slope measured through zero lift also resulted for all Mach numbers investigated (0.6 to 0.925, and 1.2 to 1.7) when the original wing was modified by bluntness at the trailing edge.

Comparison of the effects of full bluntness on the one hand, and of half bluntness on the other, upon pitching moment, lift-curve slope, and upon drag indicates that the optimum thickness for the blunt trailing edge, disregarding structural considerations, is something less than one-half the maximum thickness for the type of wing here considered. Tests of a rectangular wing of aspect ratio 4 with a 4-percent-thick circular-arc biconvex section modified in the same manner as wing 4 of this present investigation (reference 12) show that employment of a trailing-edge thickness 0.3 that of the maximum airfoil thickness gave no increase in minimum drag over that of the basic wing. This phenomenon, in conjunction with a greater lift-curve slope, produced a somewhat higher value of maximum lift-drag ratio in the subsonic speed range. The improvement in pitching-moment characteristics was comparable to that obtained with trailing-edge thicknesses 0.6 and 1.0 times the maximum airfoil thickness. Need for further investigation of the effects of trailing-edge thickness upon aerodynamic characteristics is indicated.

The fairing of the trailing-edge thickness to the circular-arc profile by means of a straight line tangent to the curved surface appears to be superior to the inclusion of a discontinuity in slope in the profile.

Data obtained in this investigation indicate that the maximum lift-drag ratios for the blunt-trailing-edge wings are increasing in value with increasing Mach number in the neighborhood of $M = 1.7$. Testing at speeds higher than this appears desirable to investigate this trend.

Ames Aeronautical Laboratory
National Advisory Committee for Aeronautics
Moffett Field, Calif.

REFERENCES

1. Reese, David E., Jr., and Phelps, E. Ray: Lift, Drag, and Pitching Moment of Low-Aspect-Ratio Wings at Subsonic and Supersonic Speeds - Plane Tapered Wing of Aspect Ratio 3.1 With 3-Percent-Thick, Biconvex Section. NACA RM A50K28, 1951.

2. Eggers, A. J., Jr.: Aerodynamic Characteristics at Subcritical and Supercritical Mach Numbers of Two Airfoil Sections Having Sharp Leading Edges and Extreme Rearward Positions of Maximum Thickness. NACA RM A7C10, 1947.

3. Lindsey, W. F., Daley, Bernard N., and Humphreys, Milton D.: The Flow and Force Characteristics of Supersonic Airfoils at High Subsonic Speeds. NACA TN 1211, 1947.

4. Chapman, Dean R.: Reduction of Profile Drag at Supersonic Velocities by the Use of Airfoil Sections Having a Blunt Trailing Edge. NACA RM A9H11, 1949.

5. Frick, Charles W., and Olson, Robert N.: Flow Studies in the Asymmetric Adjustable Nozzle of the Ames 6- by 6-foot Supersonic Wind Tunnel. NACA RM A9E24, 1949.

6. Olson, Robert N., and Mead, Merrill H.: Aerodynamic Study of a Wing-Fuselage Combination Employing a Wing Swept Back 63°. - Effectiveness of an Elevon as a Longitudinal Control and the Effects of Camber and Twist on the Maximum Lift-Drag Ratio at Supersonic Speeds. NACA RM A50A31a, 1950.

7. Glauert, H.: The Elements of Aerofoil and Airscrew Theory. The University Press, Cambridge, England, 1926, ch. XIV.

8. Herriot, John G.: Blockage Corrections for Three-Dimensional-Flow Closed-Throat Wind Tunnels, with Consideration of the Effect of Compressibility. NACA Rep. 995, 1950. (Formerly NACA RM A7B28)

9. Lessing, Henry C.: Aerodynamic Study of a Wing-Fuselage Combination Employing a Wing Swept Back 63° - Effect of Sideslip on Aerodynamic Characteristics at a Mach Number of 1.4 With the Wing Twisted and Cambered. NACA RM A50F09, 1950.

10. Perkins, Edward W.: Experimental Investigation of the Effects of Support Interference on the Drag of Bodies of Revolution at a Mach Number of 1.5. NACA TN 2292, 1951.

11. Liepmann, Hans Wolfgang: Investigations of the Interaction of Boundary Layer and Shock Waves in Transonic Flow. AF Tech. Rep. 5668, 1948.

12. Cleary, Joseph W., and Stevens, George L.: The Effects at Transonic Speeds of Thickening the Trailing Edge of a Wing With a 4-Percent-Thick Circular-Arc Airfoil. NACA RM A51J11, 1951.

Equation of fuselage radii:

$$\frac{r}{r_o} = \left[1-\left(1-\frac{2x}{l}\right)^2\right]^{3/4}$$

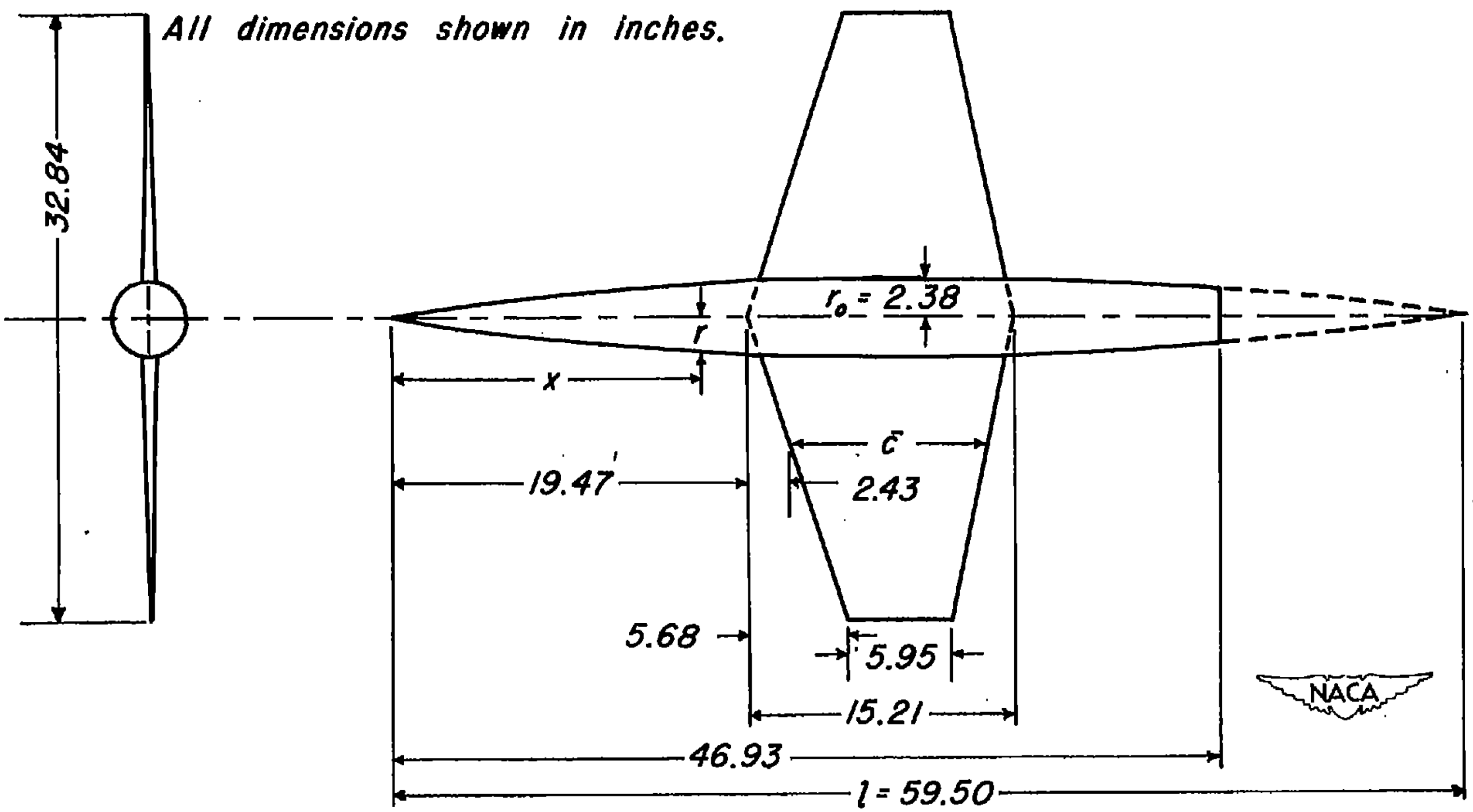

Figure 1.– Plan and front views of the models.

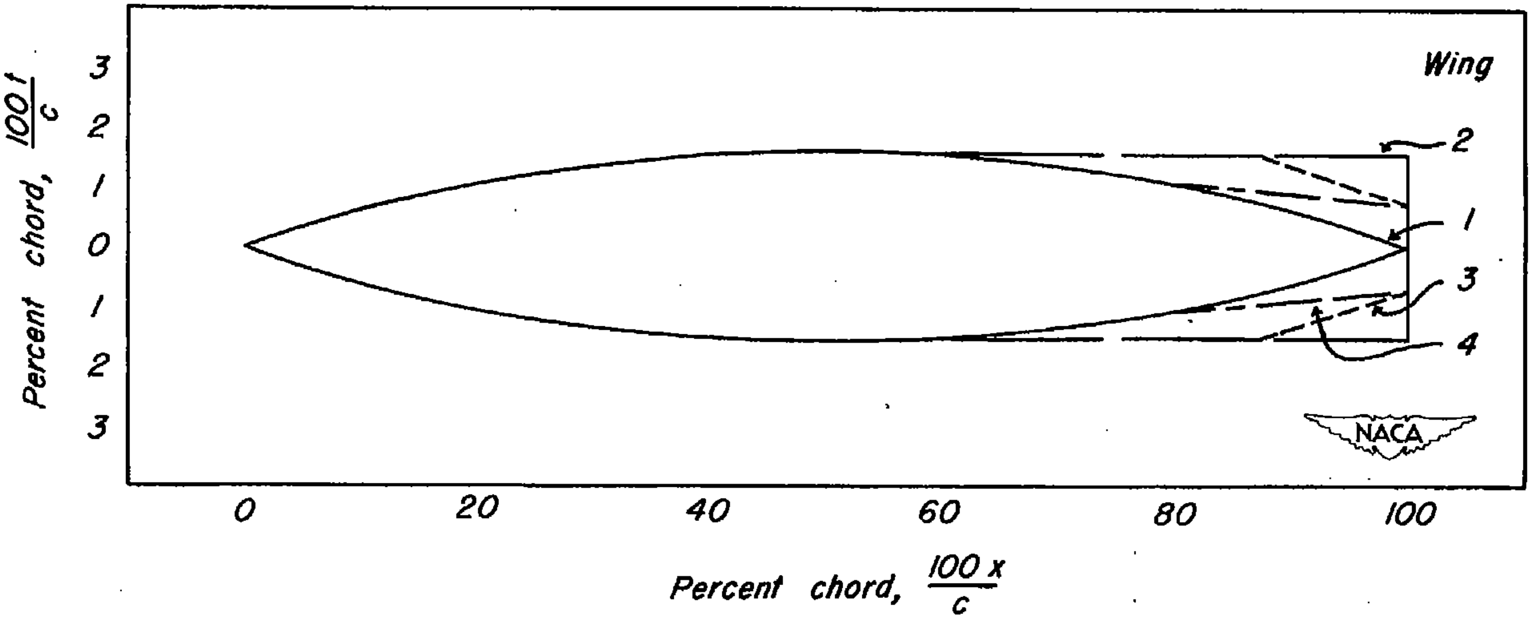

Figure 2.– Profiles of basic and blunt trailing-edge wings.

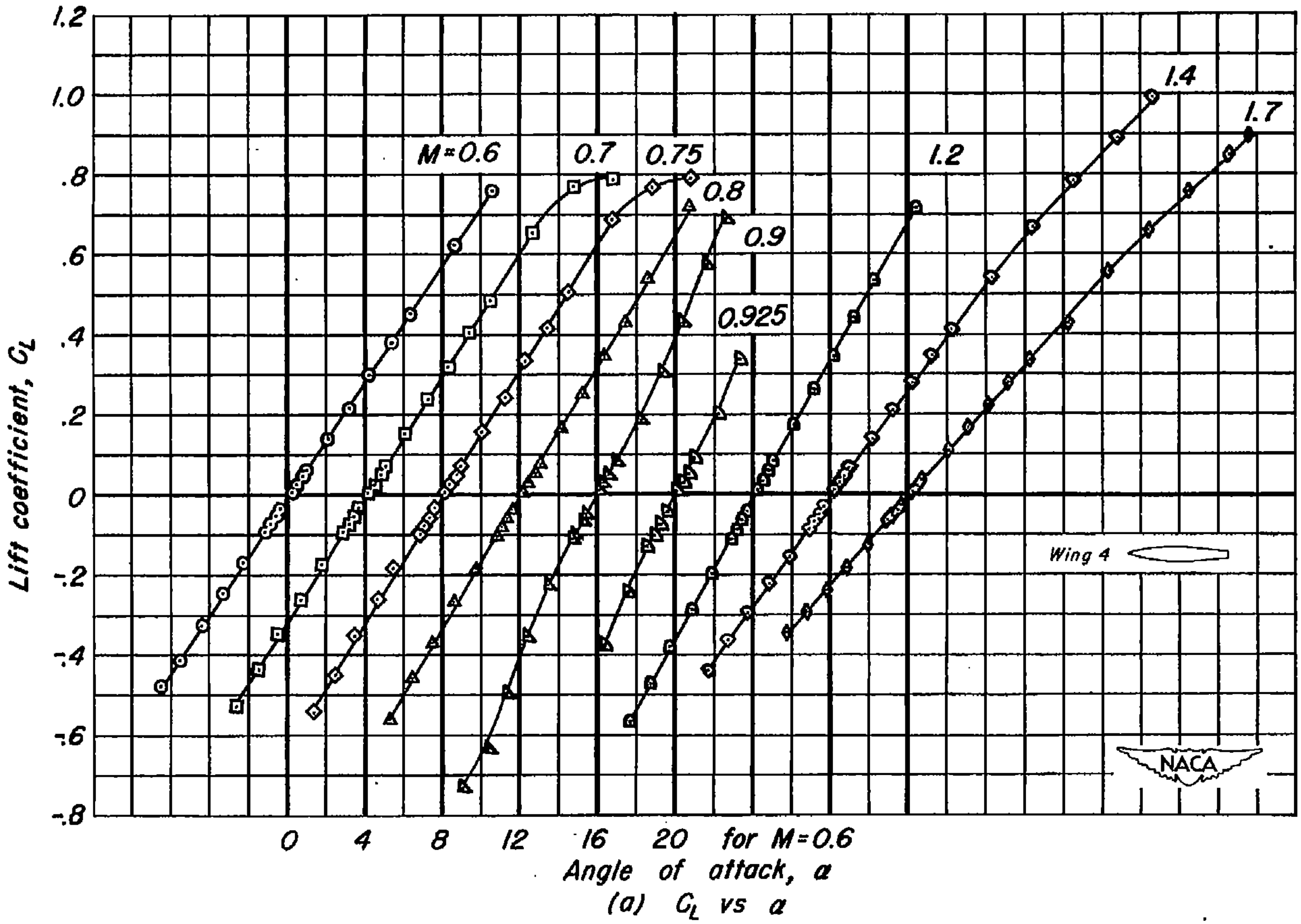

Figure 3.- The variation of the aerodynamic characteristics with lift coefficient at various Mach numbers. Reynolds number, 1.5 million, Wing 4.

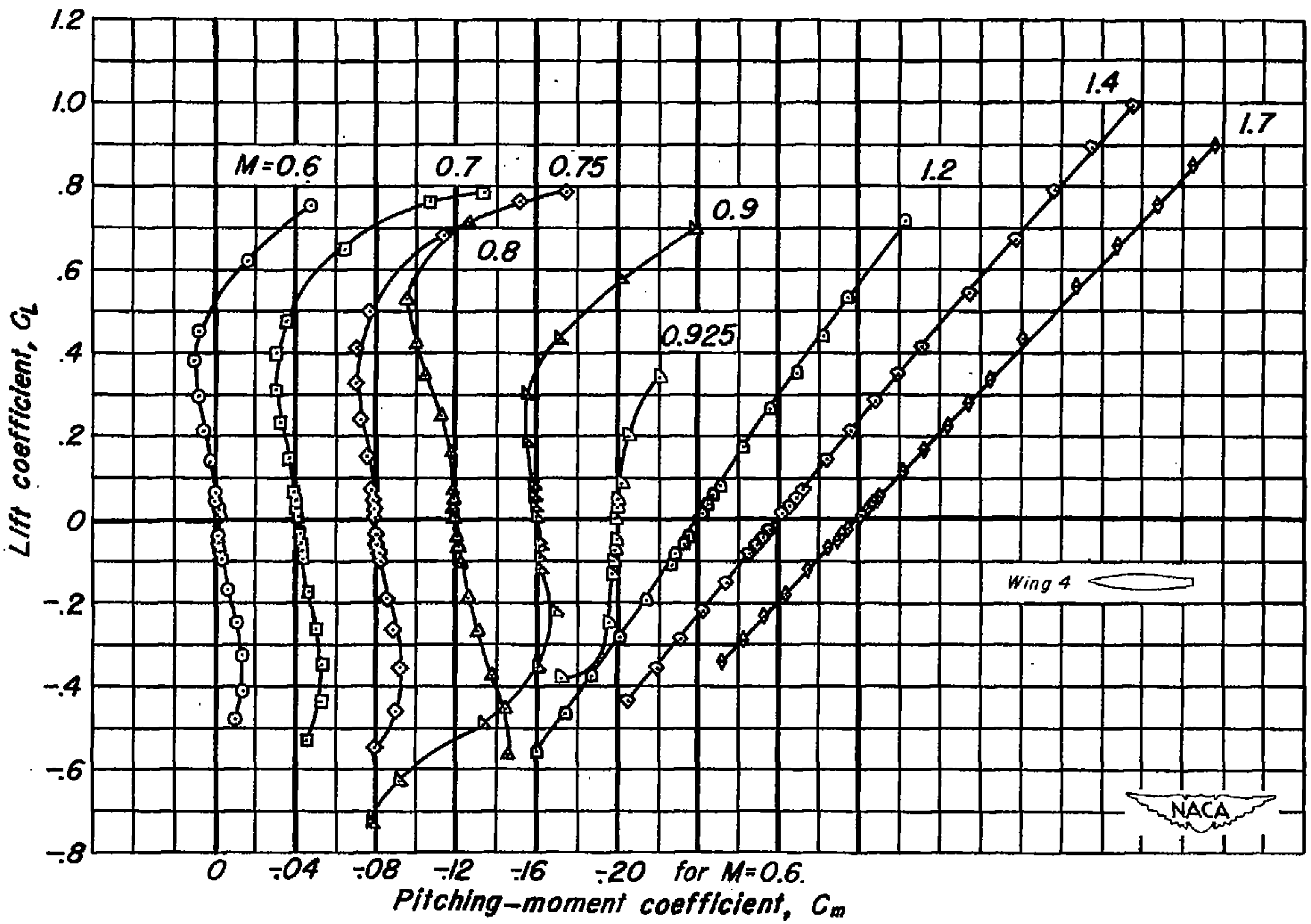

(b) C_L vs C_m

Figure 3-Continued.

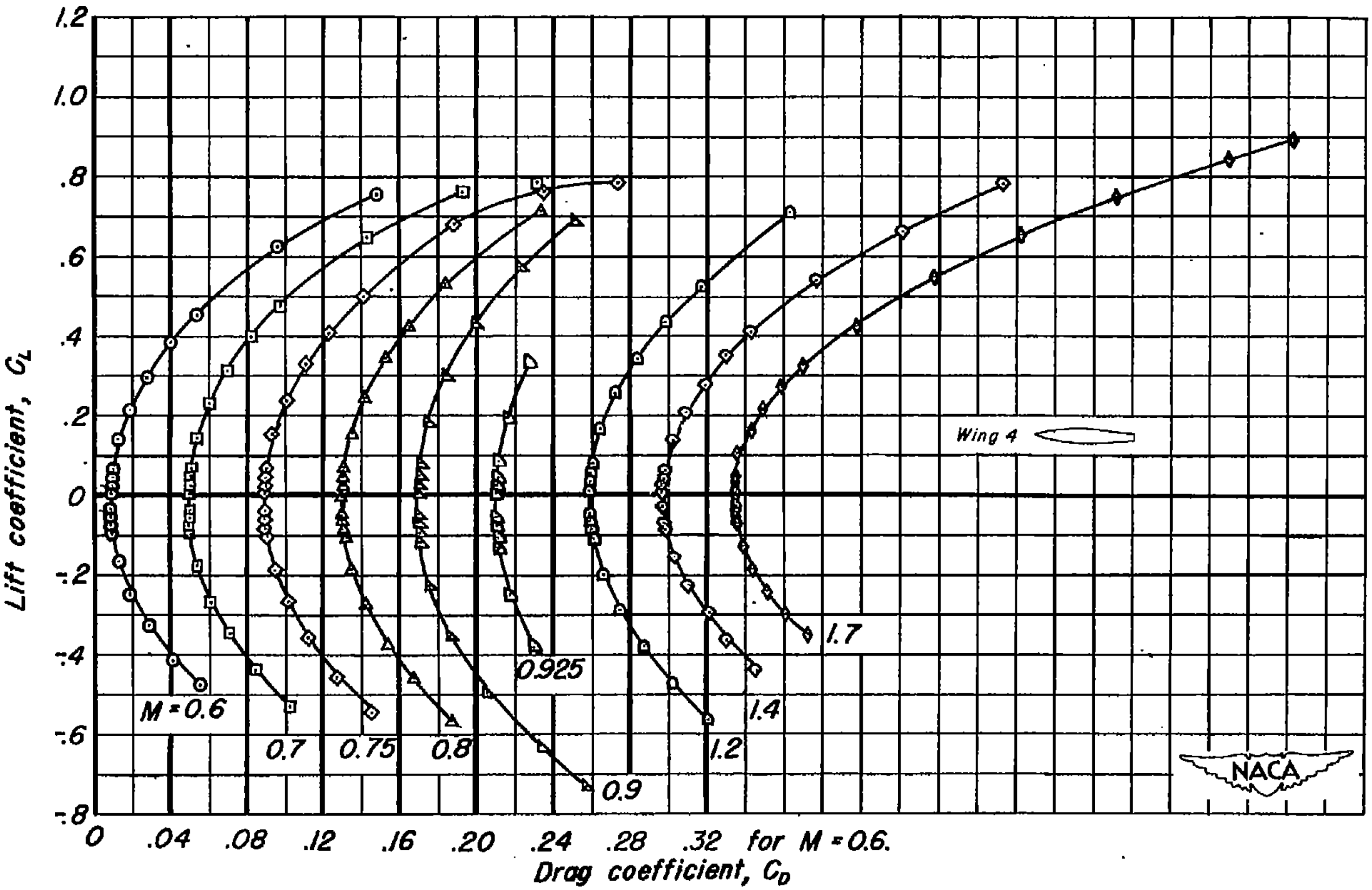

(c) C_L vs C_D

Figure 3-Continued.

[redacted]

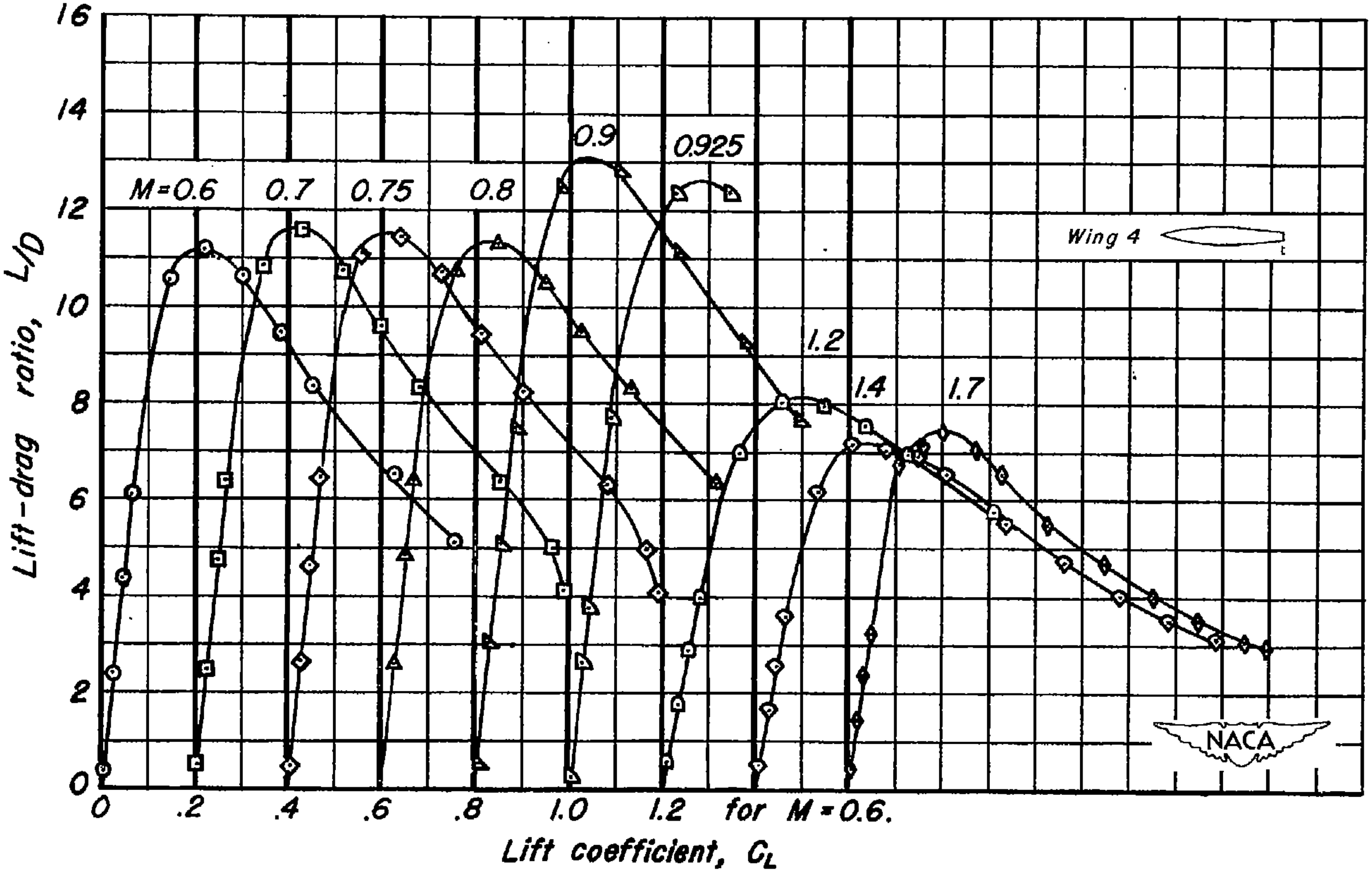

(d) L/D vs C_L

Figure 3 - Concluded.

[redacted]

[redacted]

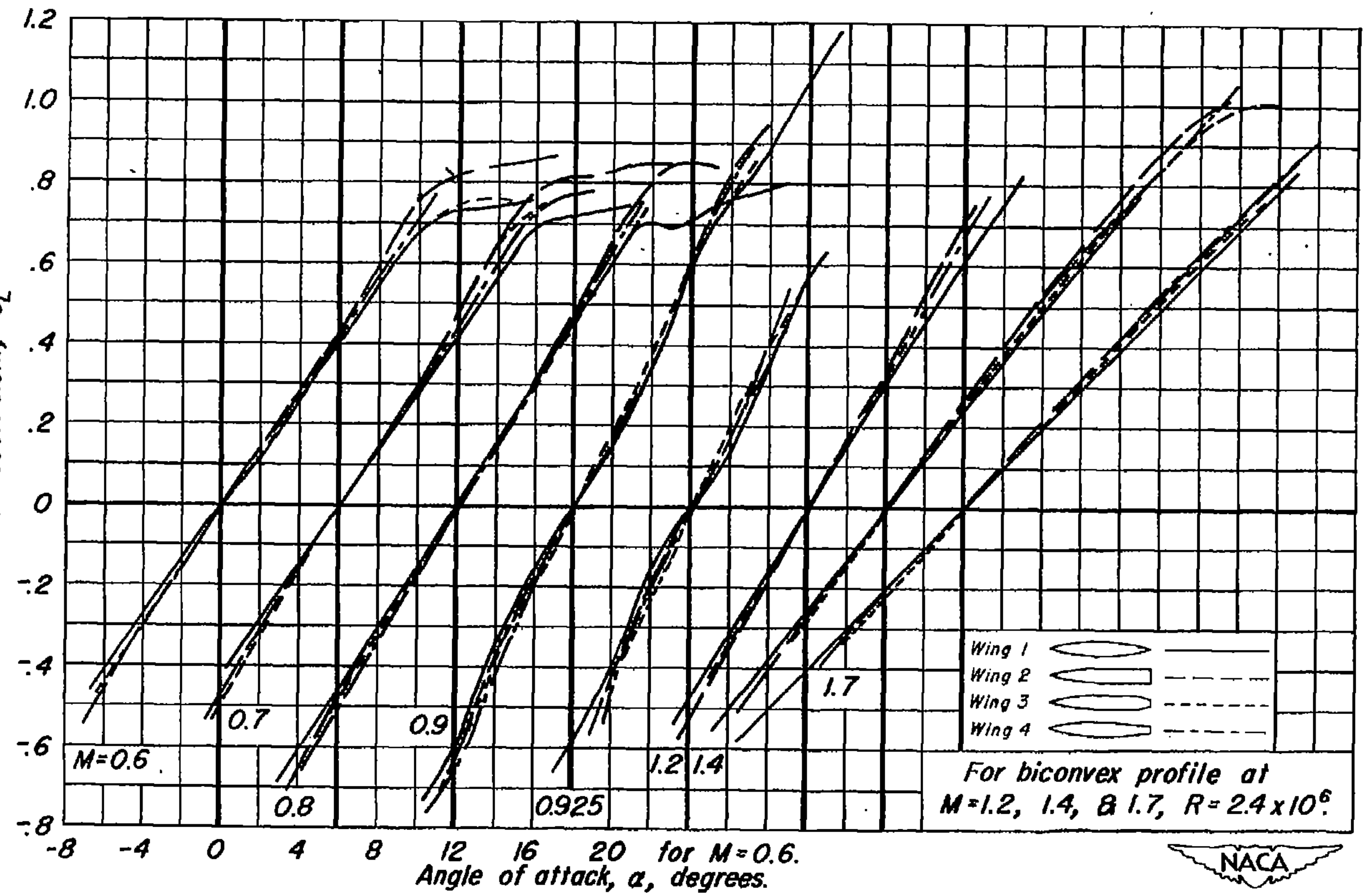

(a) Reynolds number, 1.5 million.

Figure 4.- Variation of lift coefficient with angle of attack, wings 1, 2, 3, and 4.

[redacted]

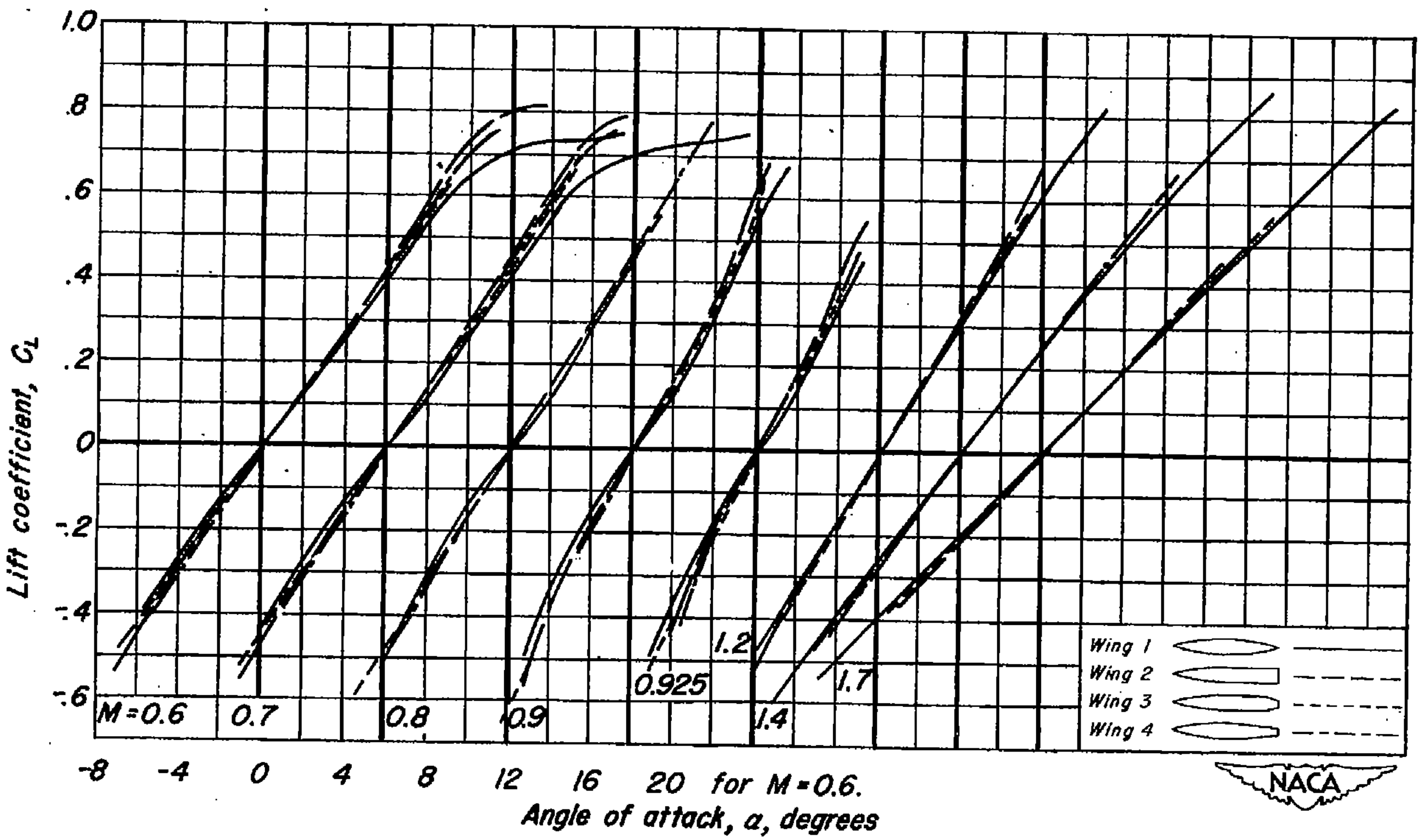

(b) Reynolds number, 3.8 million.
Figure 4 - Concluded.

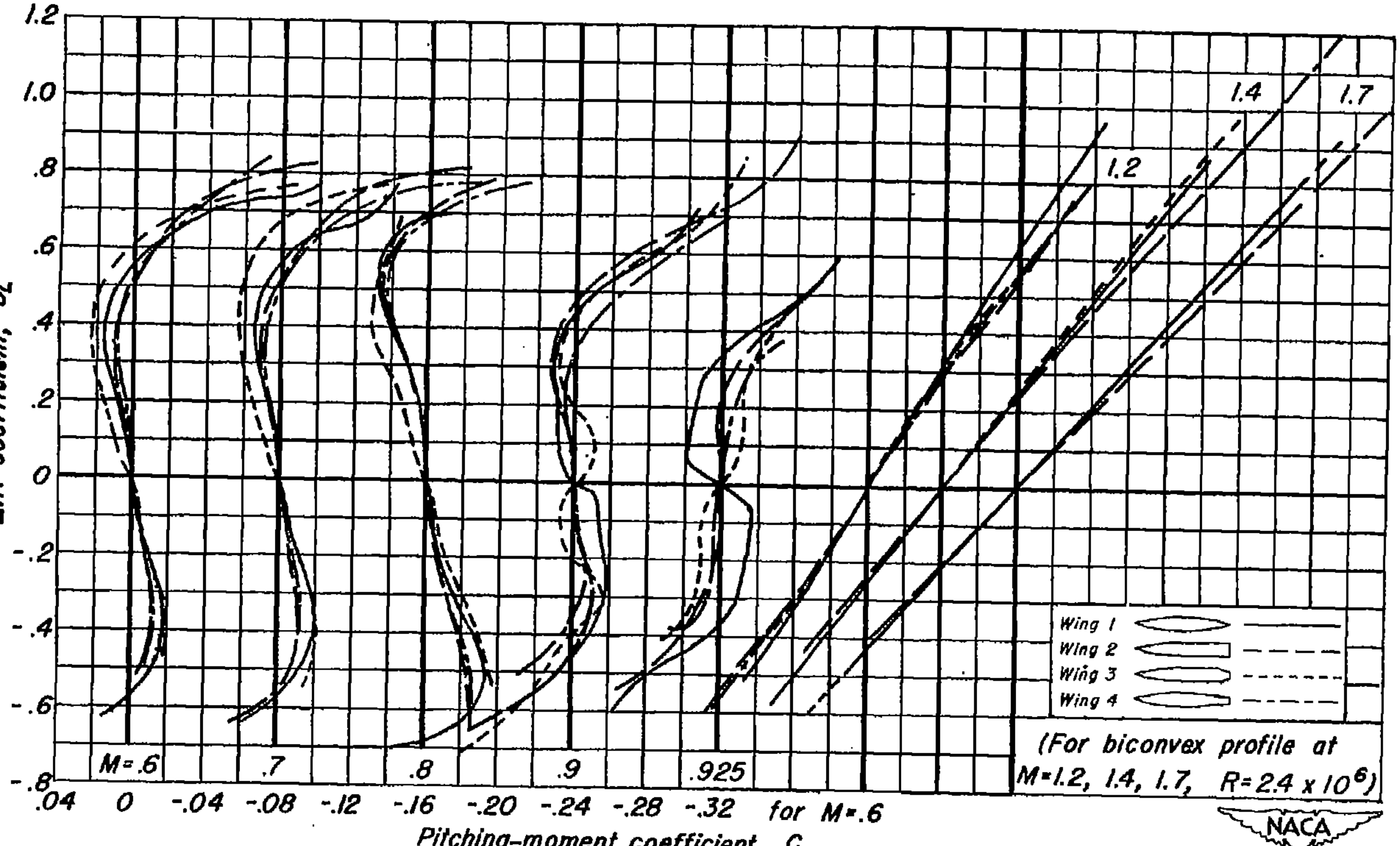

(a) Reynolds number, 1.5 million.

Figure 5. - Comparison of pitching-moment characteristics of sharp-and blunt trailing-edge wings.

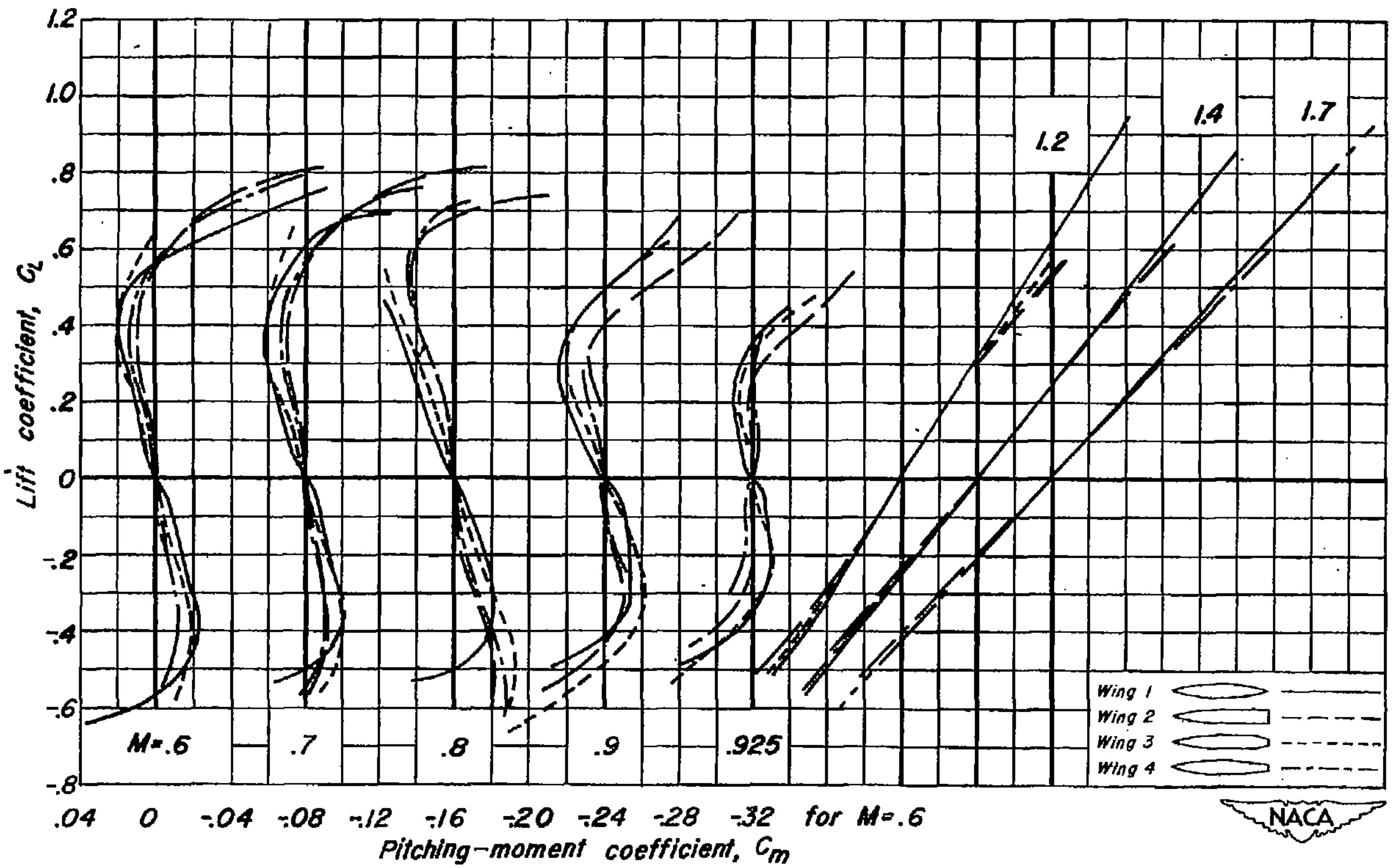

(b) Reynolds number, 3.8 million.

Figure 5.- concluded.

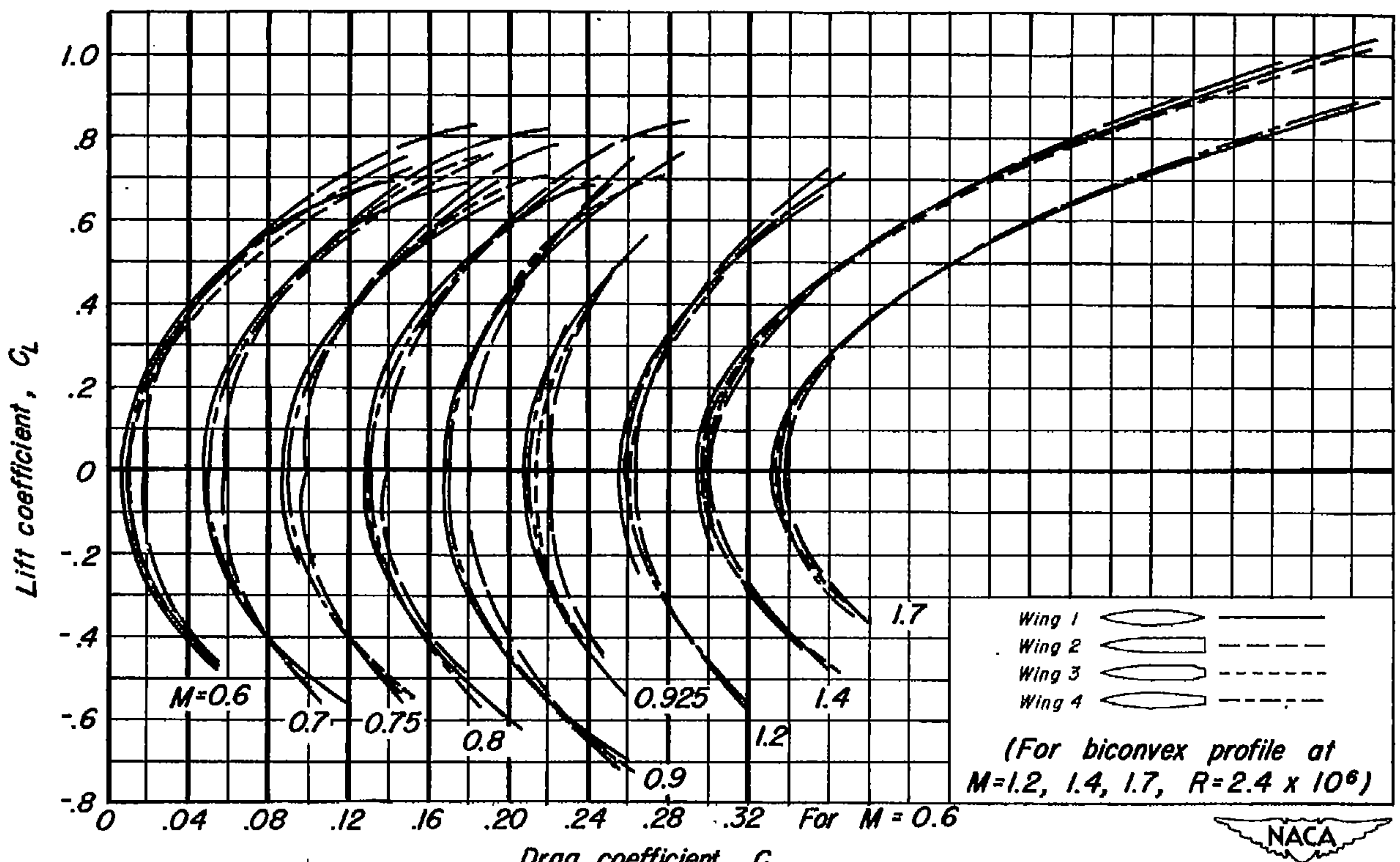

(a) Reynolds number, 1.5 million

Figure 6.– Variation of drag coefficient with lift coefficient for wings 1, 2, 3, and 4.

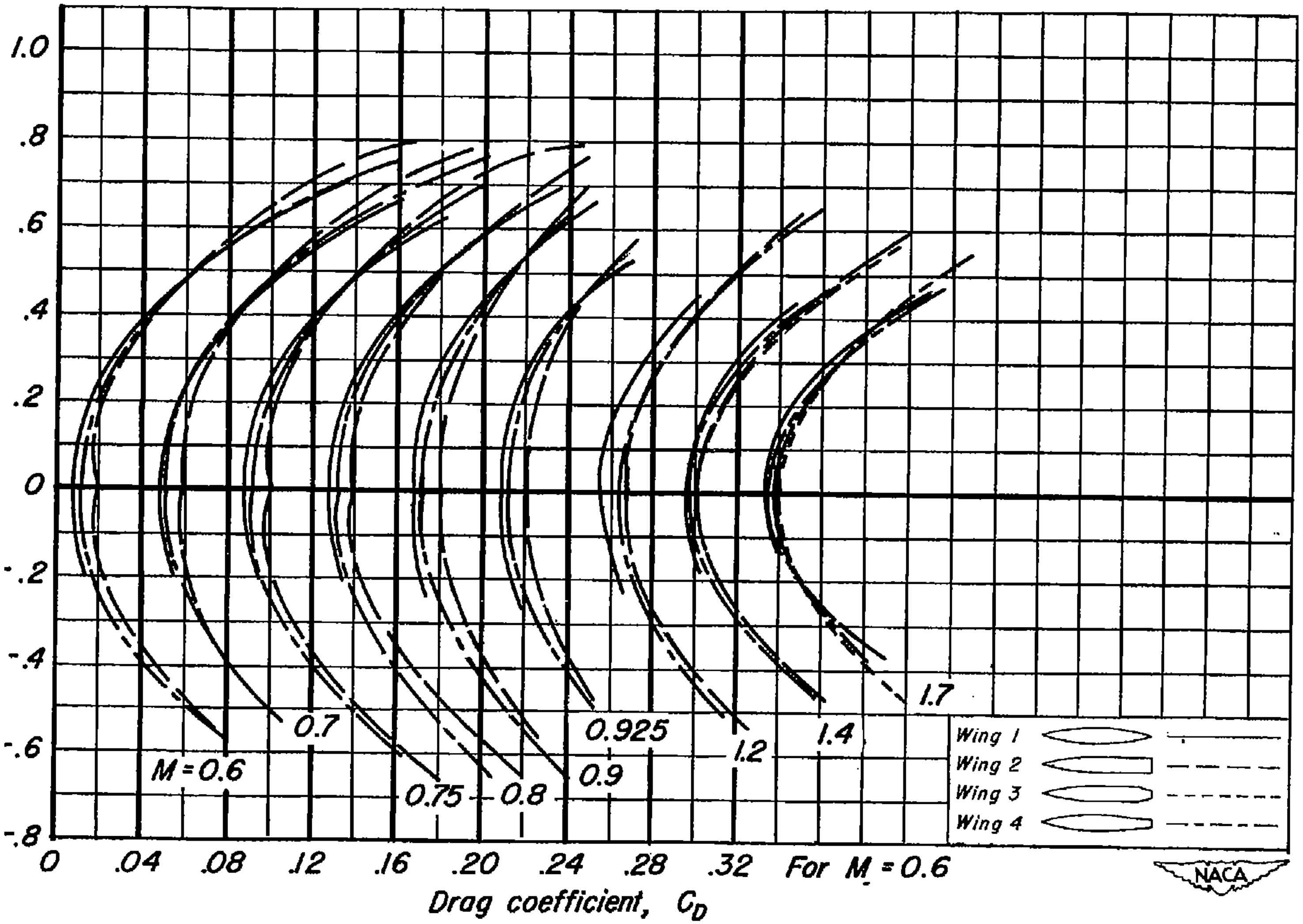

(b) Reynolds number, 3.8 million.

Figure 6.– Concluded.

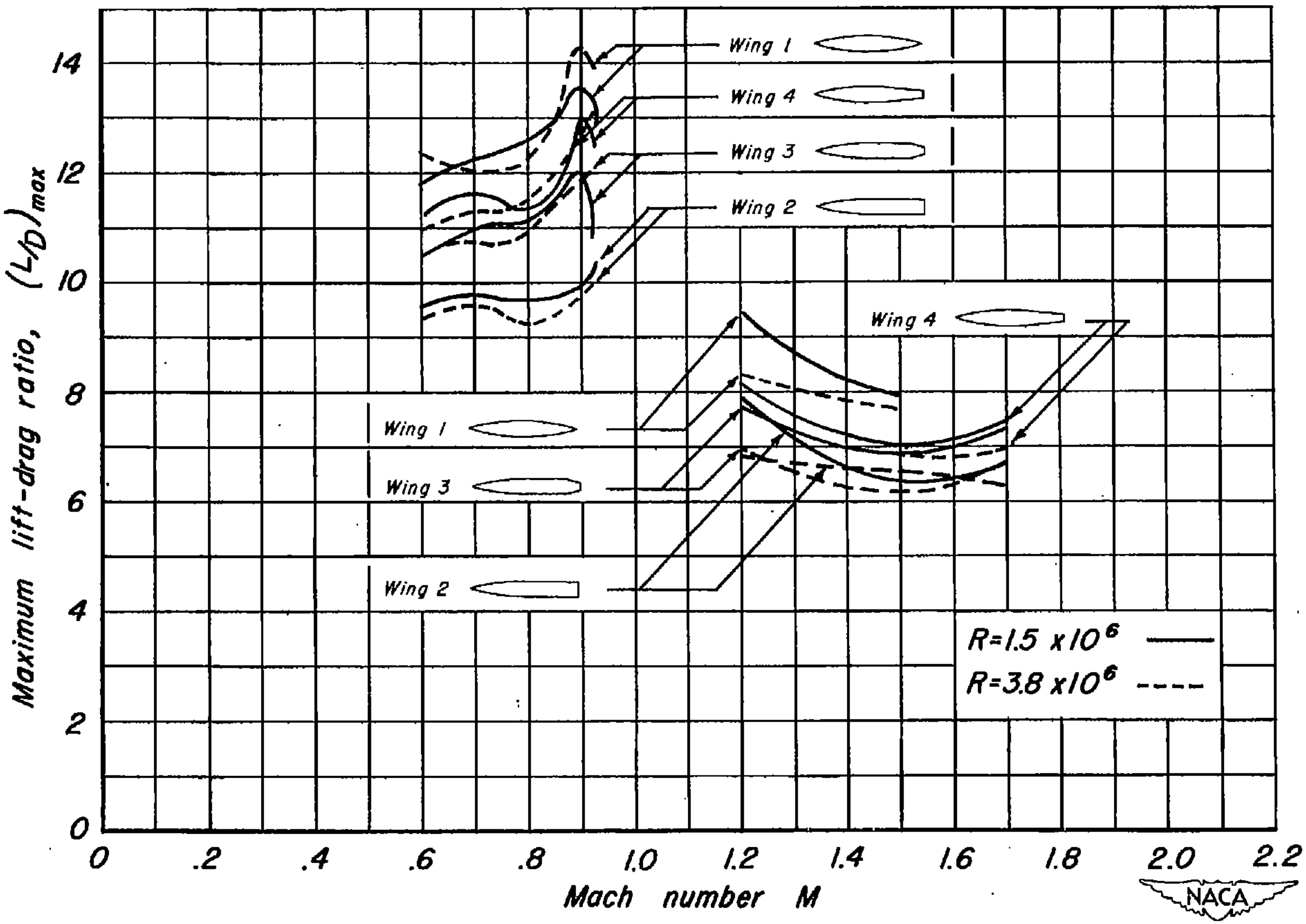

Figure 7.— Variation of maximum lift-drag ratio with Mach number, wings 1, 2, 3, and 4.

[redacted]

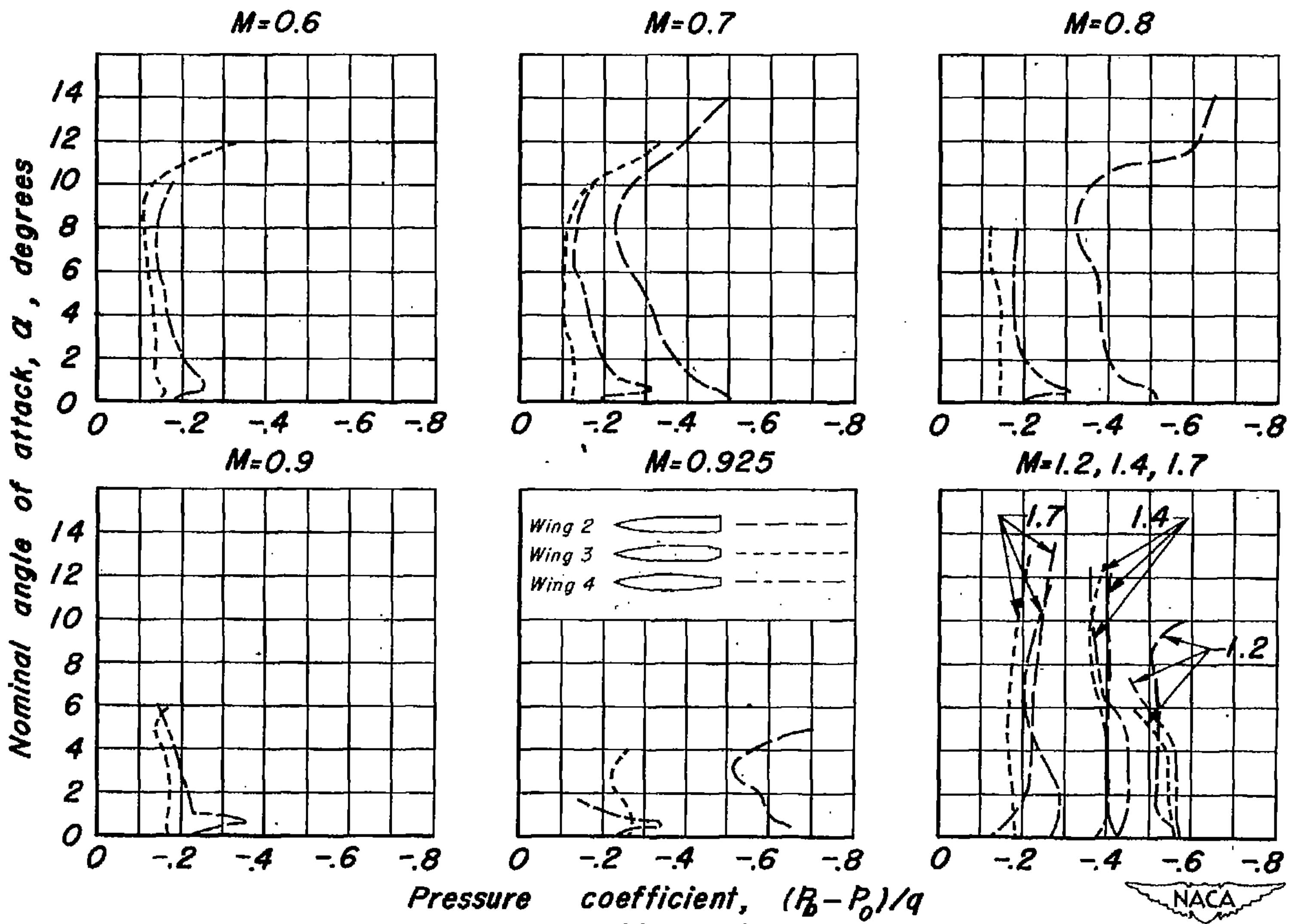

(a) Reynolds number, 1.5 million.

Figure 8.- Comparison of wing base pressure coefficients for three types of trailing-edge bluntness.

[redacted]

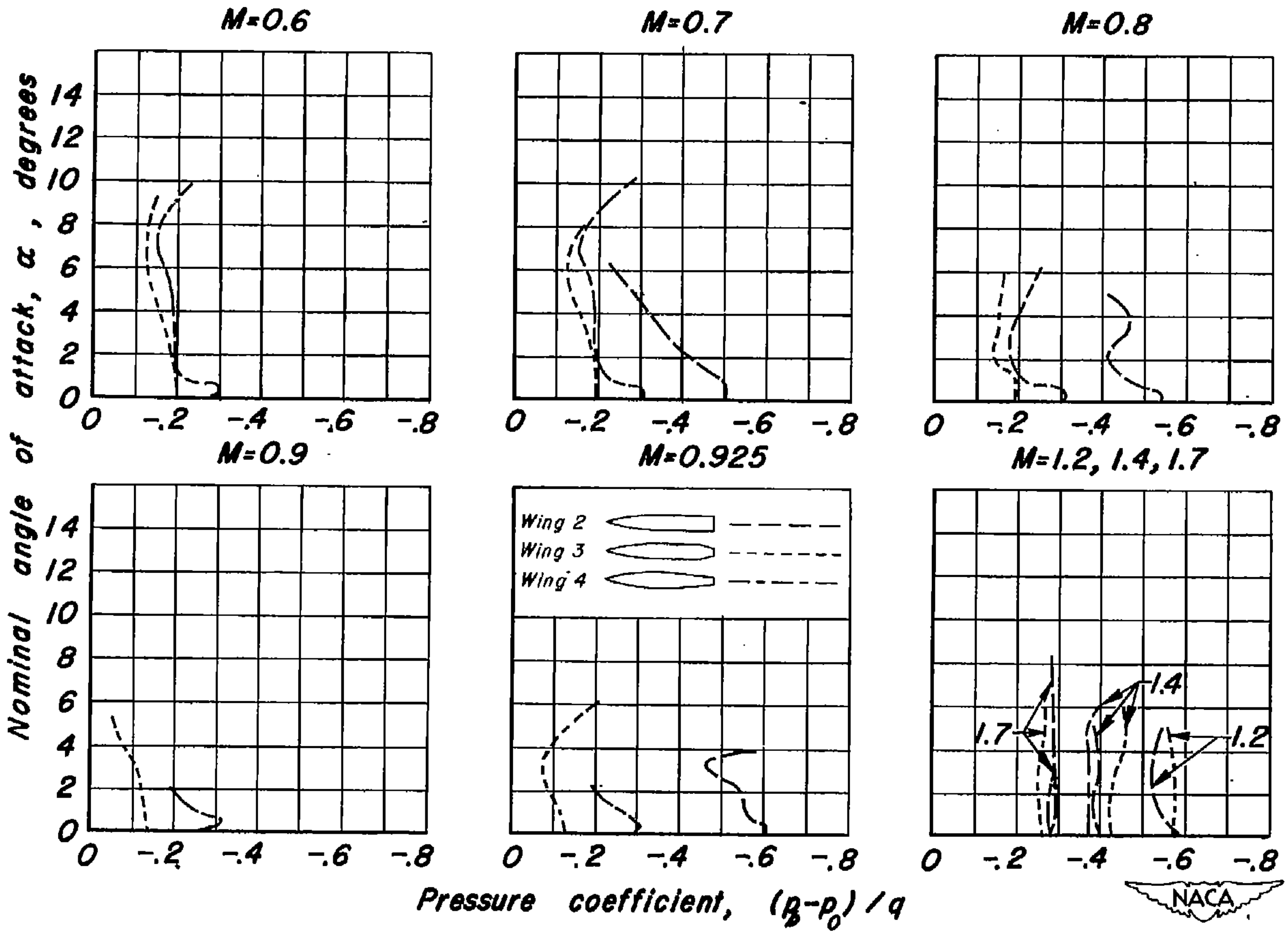

(b) Reynolds number, 3.8 million.

Figure 8.– Concluded.

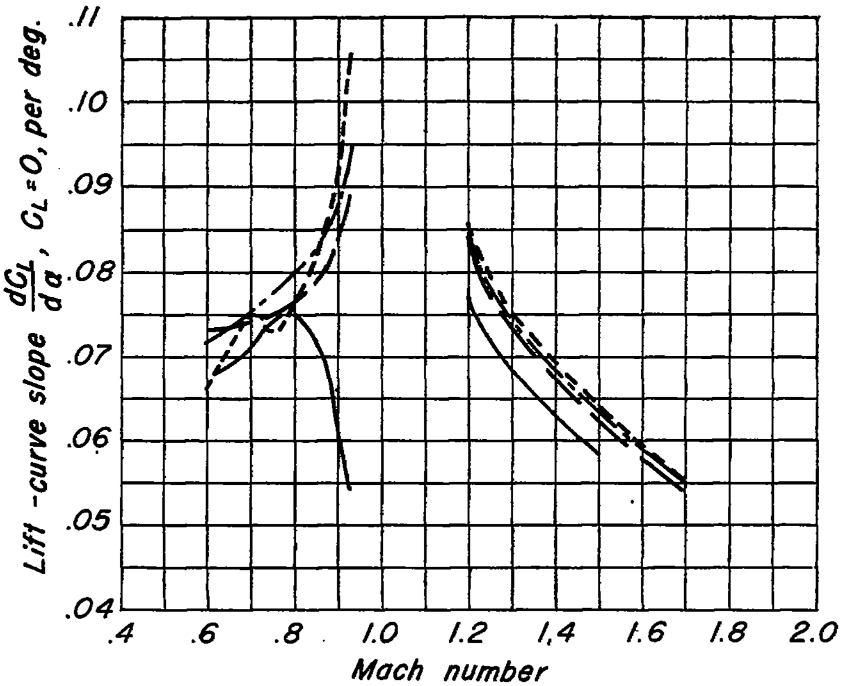

(a) Reynolds number, 1.5 million.

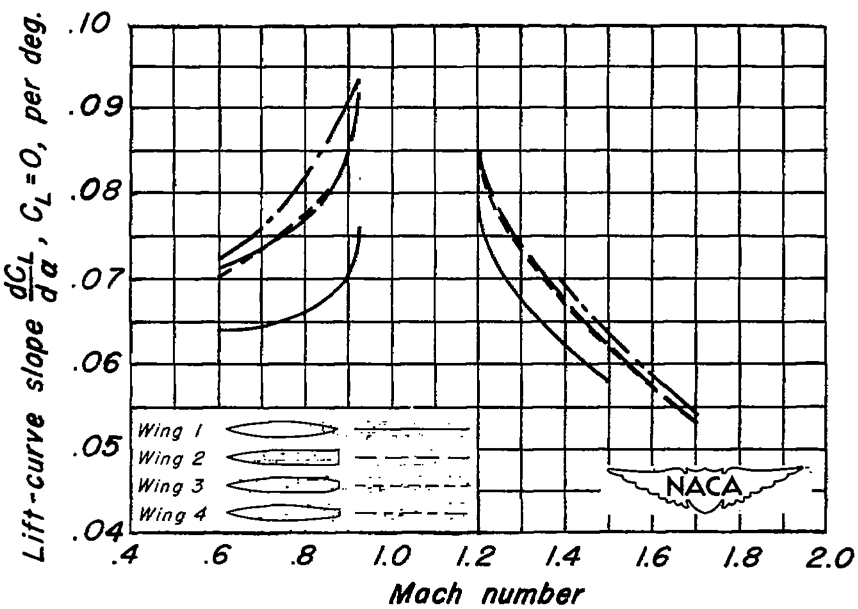

(b) Reynolds number, 3.8 million.

Figure 9. Variation of lift-curve slope with Mach number, wings 1, 2, 3, and 4.

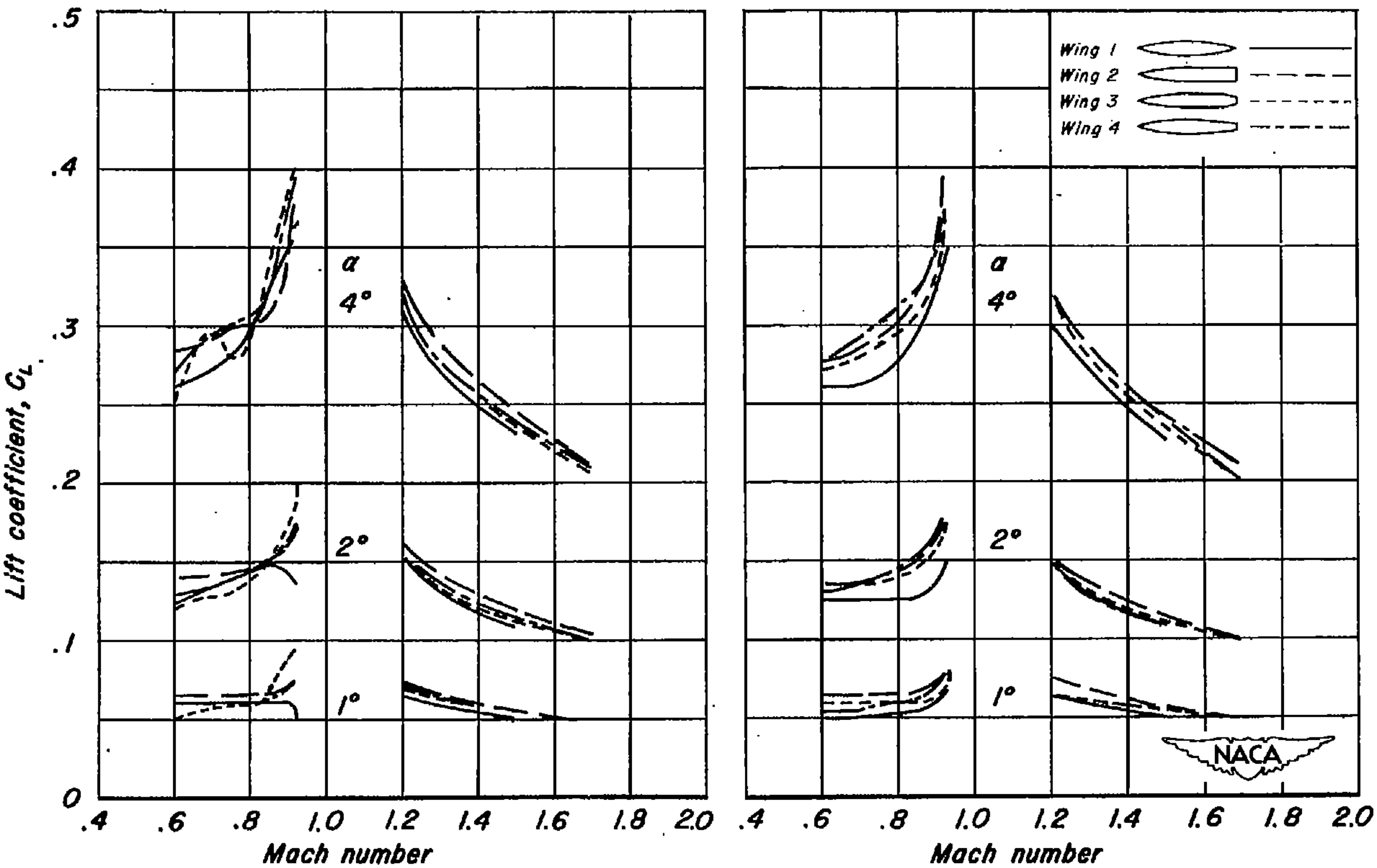

(a) Reynolds number, 1.5 million. (b) Reynolds number, 3.8 million.

Figure 10.- Variation of lift coefficient at several angles of attack with Mach number, wings 1, 2, 3, and 4.

[redacted]

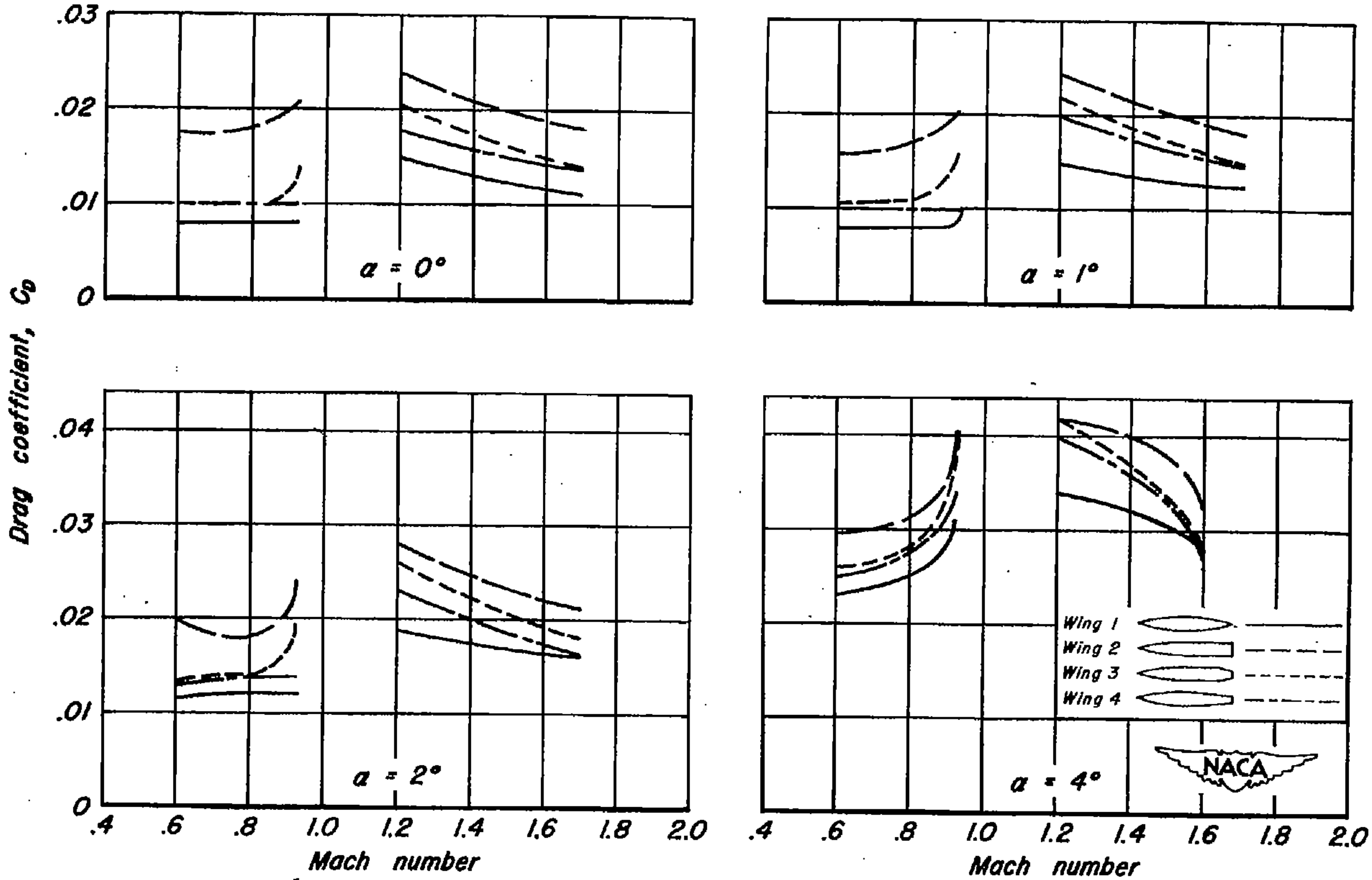

(a) Reynolds number, 1.5 million.

Figure 11.– Variation of drag coefficient at several angles of attack with Mach number, wings 1, 2, 3, and 4.

[redacted]

[redacted]

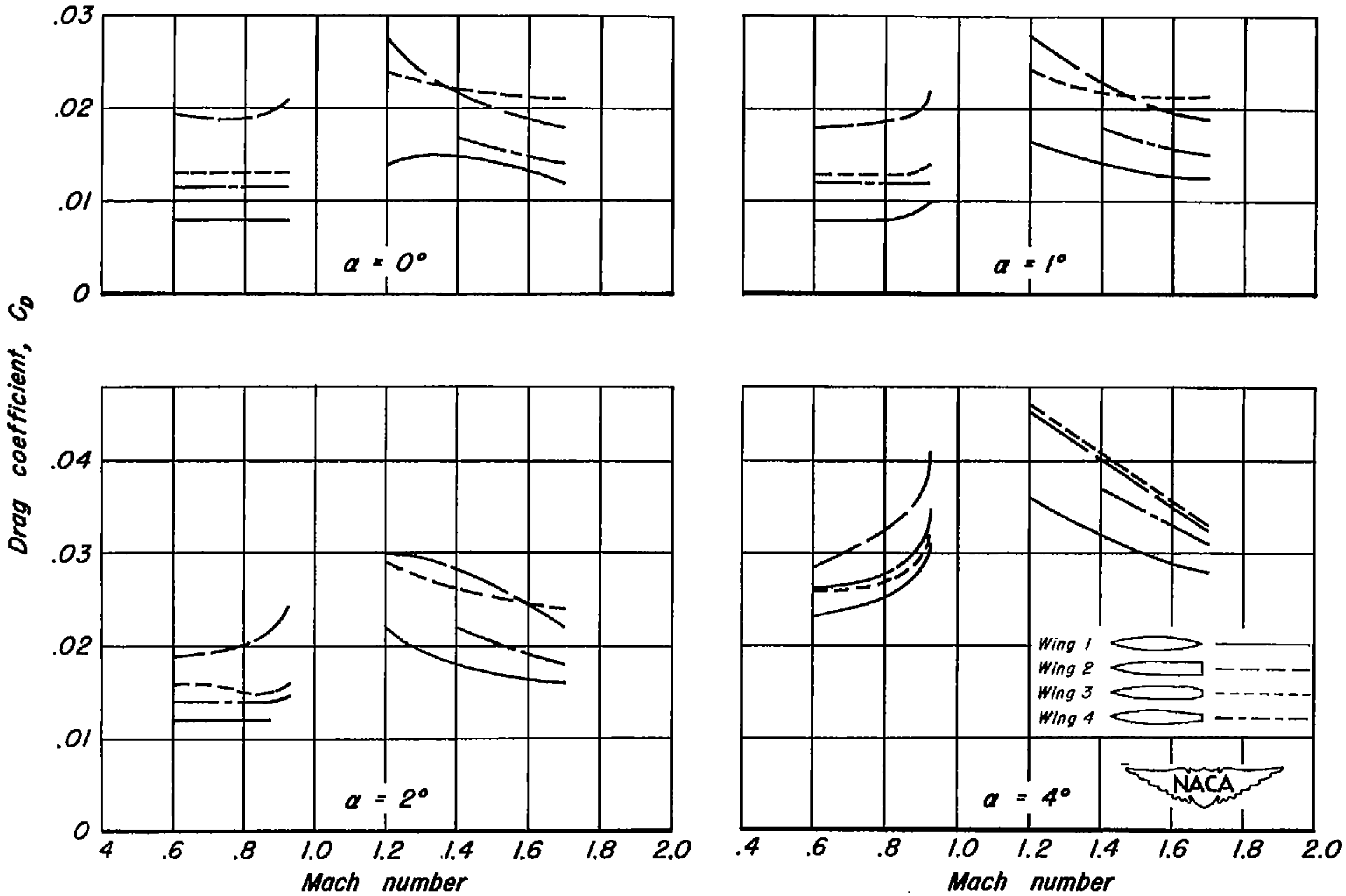

(b) Reynolds number, 3.8 million.

Figure 11.– Concluded.

[redacted]

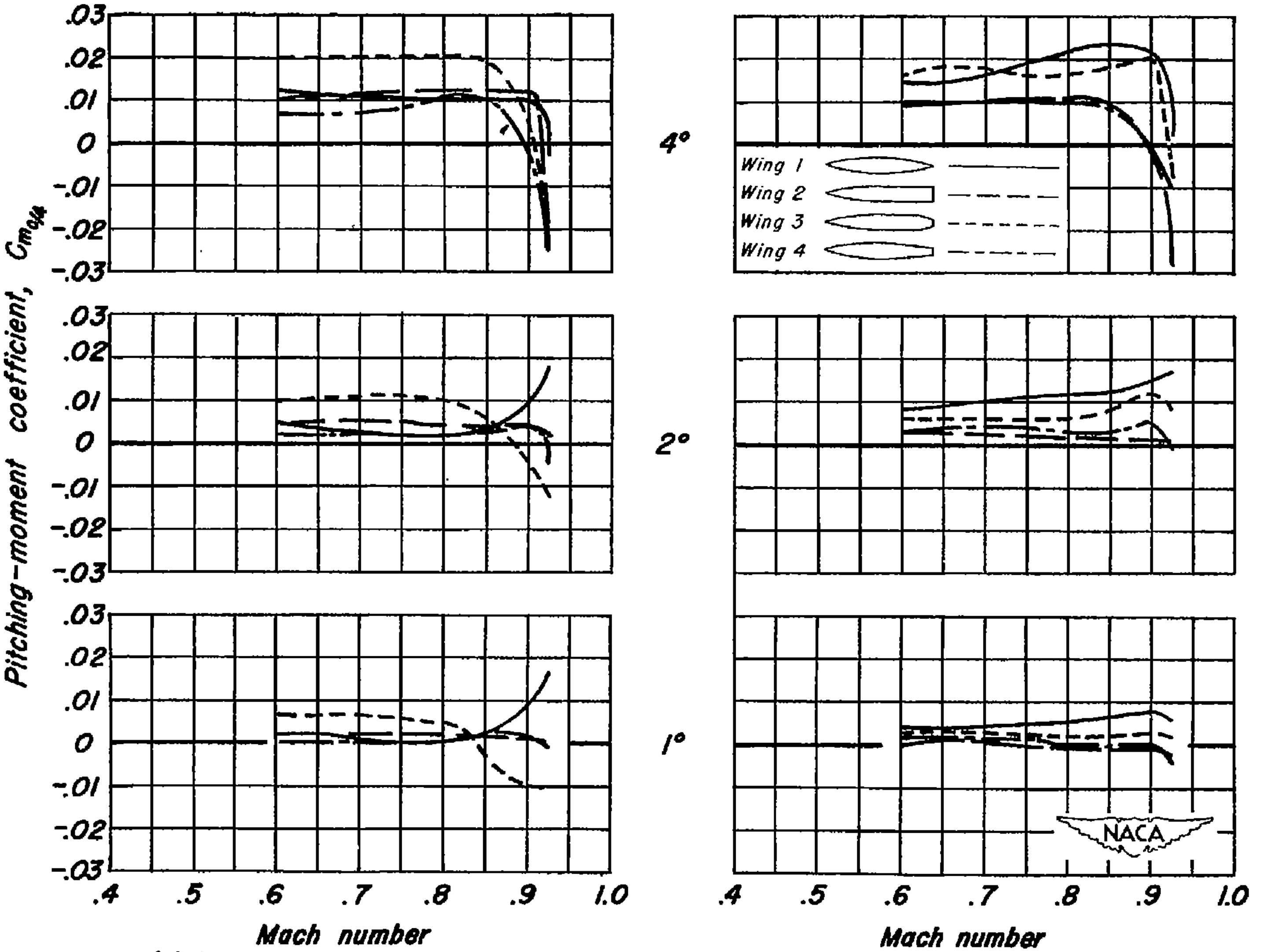

(a) Reynolds number, 1.5 million.

(b) Reynolds number, 3.8 million.

Figure 12 - Variation of pitching-moment coefficient with Mach number, wings 1, 2, 3, and 4.

[redacted]